Electronic Supplementary Information

Construction of Metal–Organic Frameworks ZIF-8-derived Heterostructure ZnO/$BiVO_4$ for Enhanced Photocatalytic Degradation of Carbamazepine

Wei Tan [a,d], Guijuan Hu [a,d], Limei Tuo [a,d], Weiyuan Zuo [a,b,*], Qi Liu [a], Haijuan Tong [b,*], Zhengjie Zhu [b], Bingfang Shi [a,c,*]

[a] Department of Food and Chemical Engineering, Liuzhou Institute of Technology, Liuzhou 545616, P.R. China

[b] Guangxi Key Laboratory of Urban Water Environment, College of Chemistry and Environmental Engineering, Baise University, Baise 533000, P.R. China

[c] School of Civil Engineering, Guangxi Transport Vocational and Technical College, Nanning 530000, P.R. China

[d] Liuzhou Key Laboratory of Plant-derived Ingredients of Liuzhou snails rice noodle, Liuzhou Institute of Technology, Liuzhou 545616, P.R. China

*Corresponding Author:

Weiyuan Zuo, E-mail: zwy1987.ok@163.com

Tel: +86-776-2848132; Fax: +86-776-2848132

Haijuan Tong, E-mail: 373946527@qq.com

Bingfang Shi, E-mail: shibingfang@126.com

Section 1: Experimental

Chemicals and materials

Carbamazepine (CBZ), $Bi(NO_3)_3 \cdot 5H_2O$, NH_4VO_3, and $Zn(NO_3)_2 \cdot 6H_2O$ were obtained from Aladdin Chemistry Co., Ltd. (Shanghai, China). HNO_3 and 2-methylimidazole were purchased from Sinopharm Chemical Reagent Co. (Shanghai, China). Methanol was obtained from Fuyu Fine Chemical Co. (Tianjin, China). All chemical reagents were of analytical grade and were used directly without further treatment.

Characterization

The X-ray diffraction (XRD) patterns of the as-prepared samples were obtained using a Rigaku Ultima IV diffractometer with Cu K_{α} radiation. Transmission electron microscopy (TEM) was performed using a FEI Tecnai G2F20 electron microscope (Hillsboro, OR, USA). X-ray photoelectron spectroscopy (XPS) was performed using a Kratos XSAM 800 photoelectron spectrometer (Manchester, UK). N_2 adsorption–desorption experiment was performed on 3-Flex automated gas sorption analyzer at 77 K. The surface area and pore-size-distribution curves were calculated using Brunauer-Emmett-Teller (BET) model and DFT method, respectively. Photoluminescence (PL) was measured using FL7000 (Hitachi, Japan). UV-vis diffuse reflectance spectra (UV-vis DRS) were recorded using a UV-3600 instrument (Shimadzu, Japan). The electrochemical impedance spectra (EIS) and photocurrent were measured on an electrochemical workstation (CHI660E, China) using a three-electrode cell system.

The intermediates of CBZ were identified by a Shimadzu 20AD LC coupled with AB Sciex 5600 hybrid quadrupole TOF-MS/MS in the positive electrospray ionization mode with a scan range of m/z 50~500. Chromatographic separation was determined with a C18 column (4.6×150 mm, 5 μm). The flow rate was 0.3 mL/min, and the injection volume was 2 μL.

Section 2: Figures

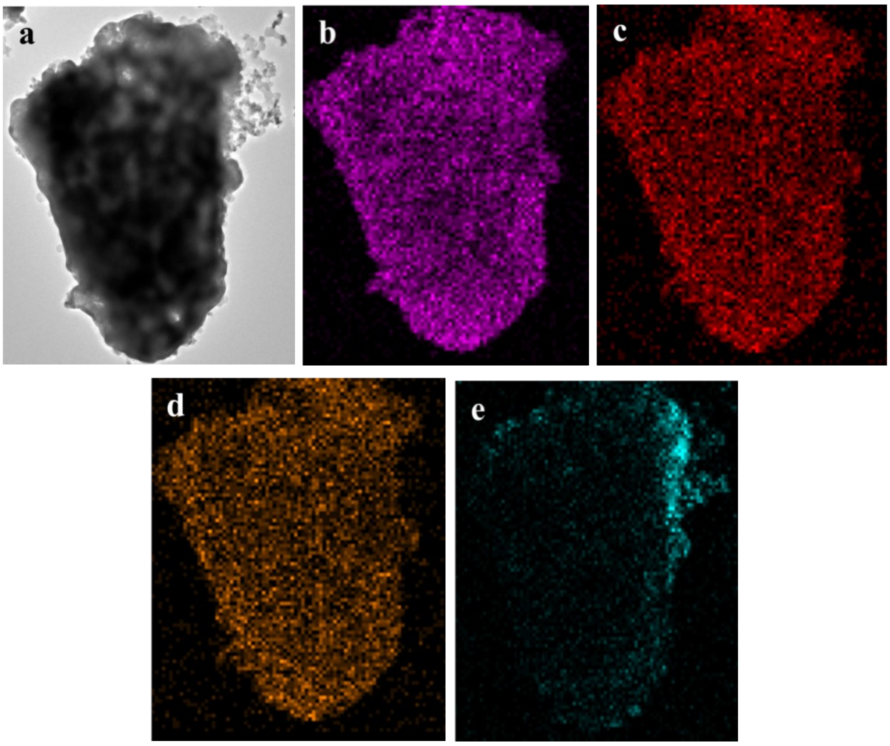

Figure S1. Elemental mapping images of $ZnO/BiVO_4$ structures: (a) the test area and element distribution of (b) Bi, (c) O, (d) V, and (e) Zn.

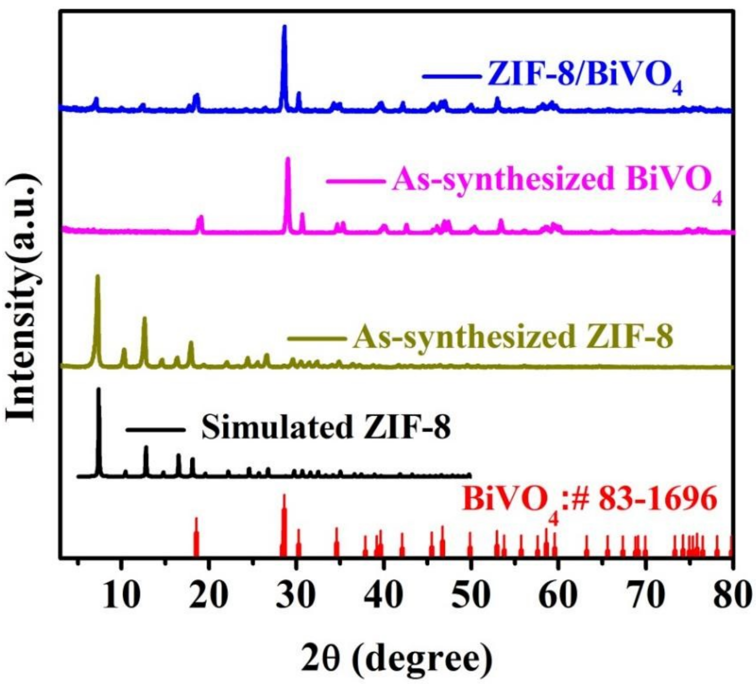

Figure S2. XRD patterns of ZIF-8 and ZIF-8-$BiVO_4$.

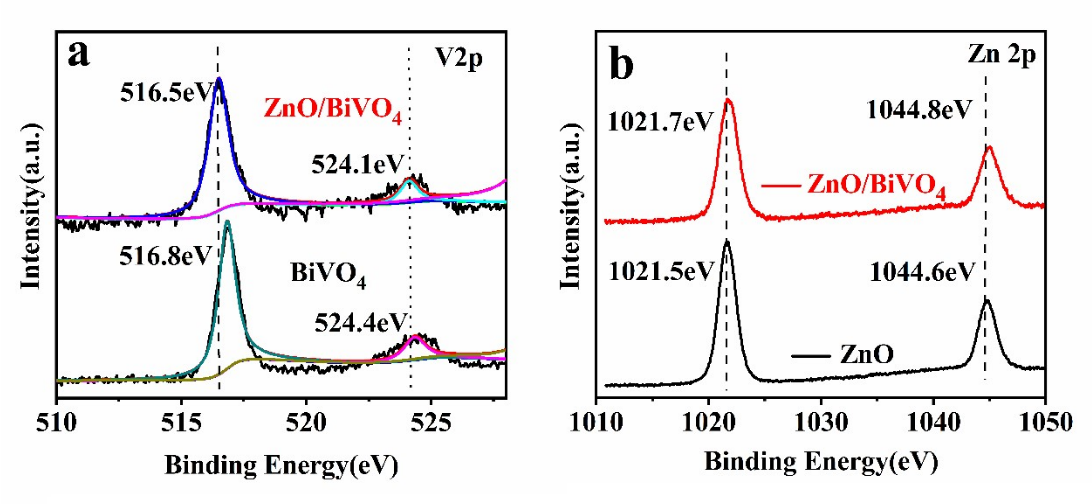

Figure S3. XPS spectrum of the as-prepared samples. (a) V 2p and (b) Zn 2p.

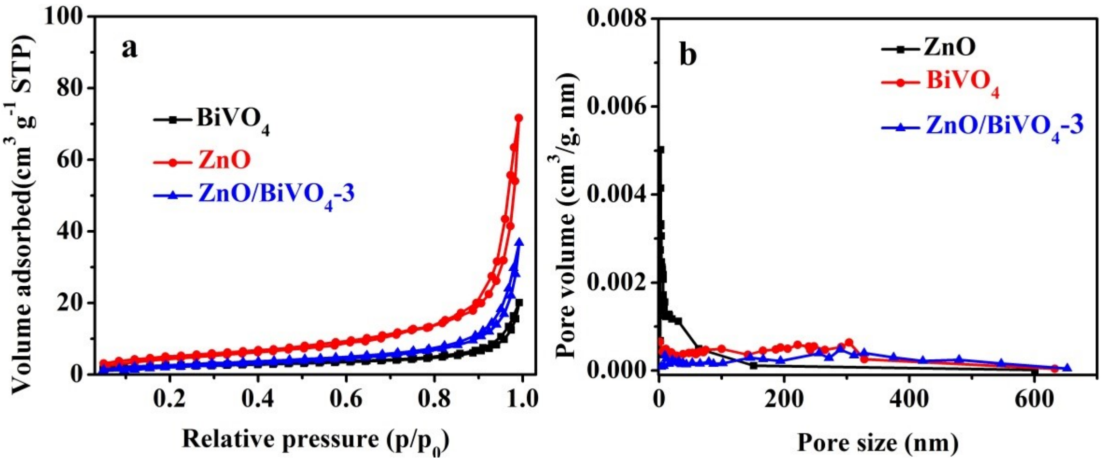

Figure S4. (a) N_2 adsorption-desorption isotherms and (b) pore size distributions of ZnO, $BiVO_4$ and ZnO/$BiVO_4$-3 samples.

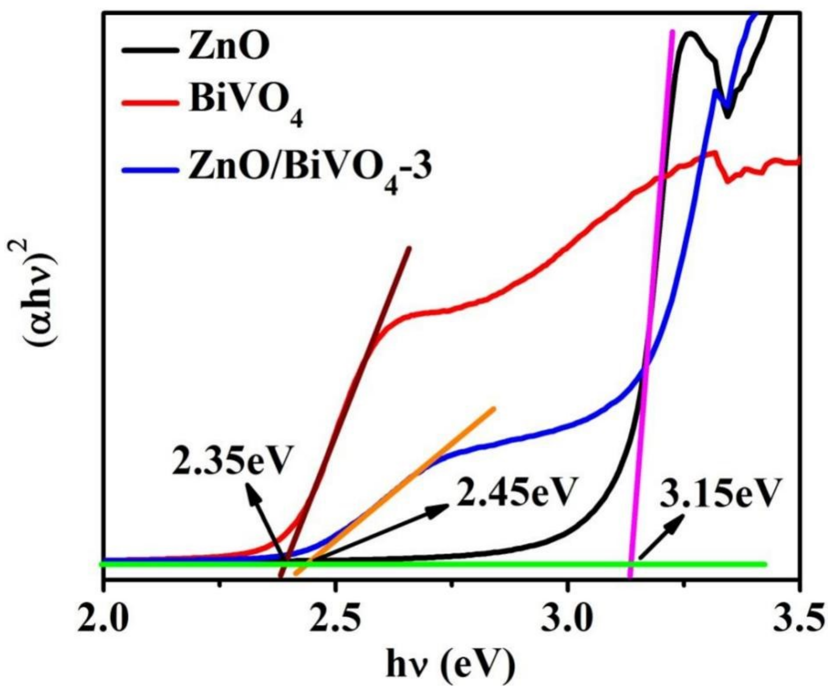

Figure S5. Tauc plots of prepared samples.

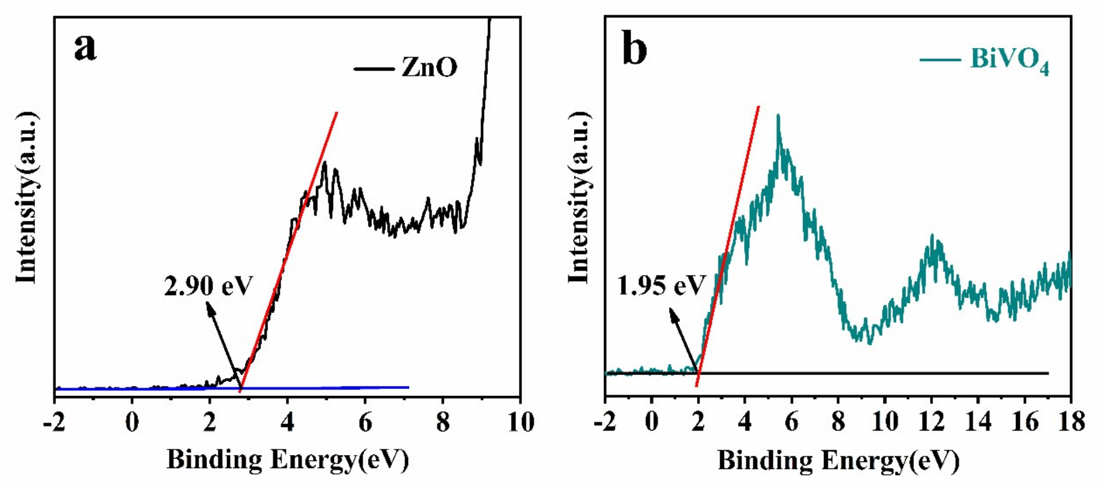

Figure S6. The VB-XPS of as-prepared (a) ZnO and (b) $BiVO_4$.

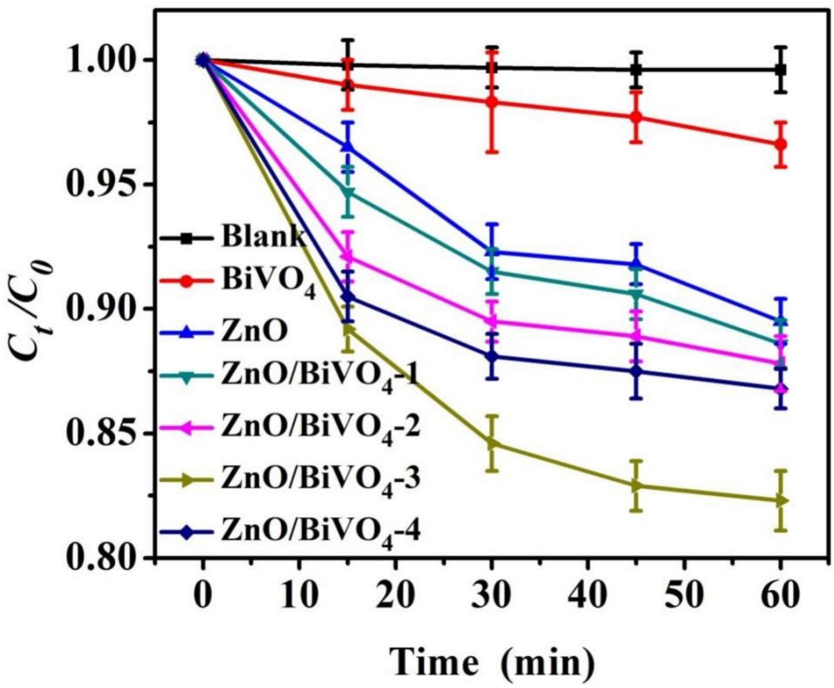

Figure S7. The adsorption of CBZ on as-prepared ZnO, $BiVO_4$ and ZnO/$BiVO_4$ composites.

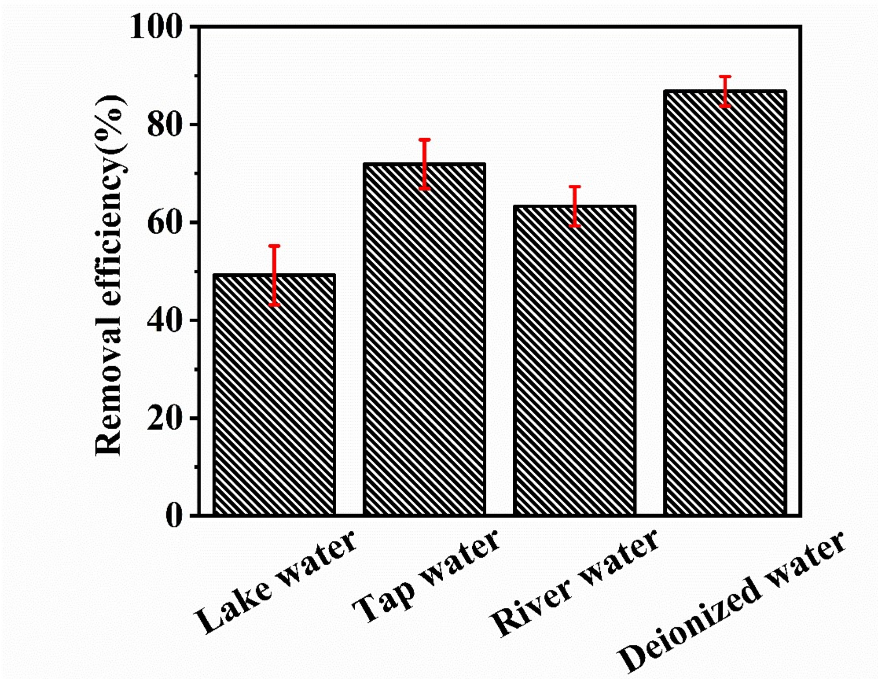

Figure S8. Evaluating the practical application of $ZnO/BiVO_4$-3.

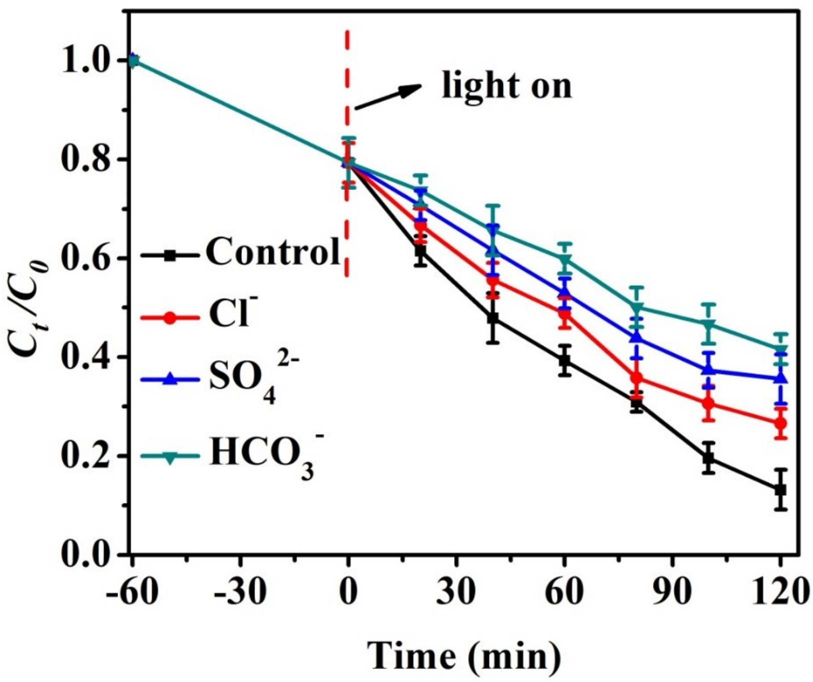

Figure S9. Effect of co-existing ions on the photocatalytic degradation of CBZ in the presence of $ZnO/BiVO_4$-3.

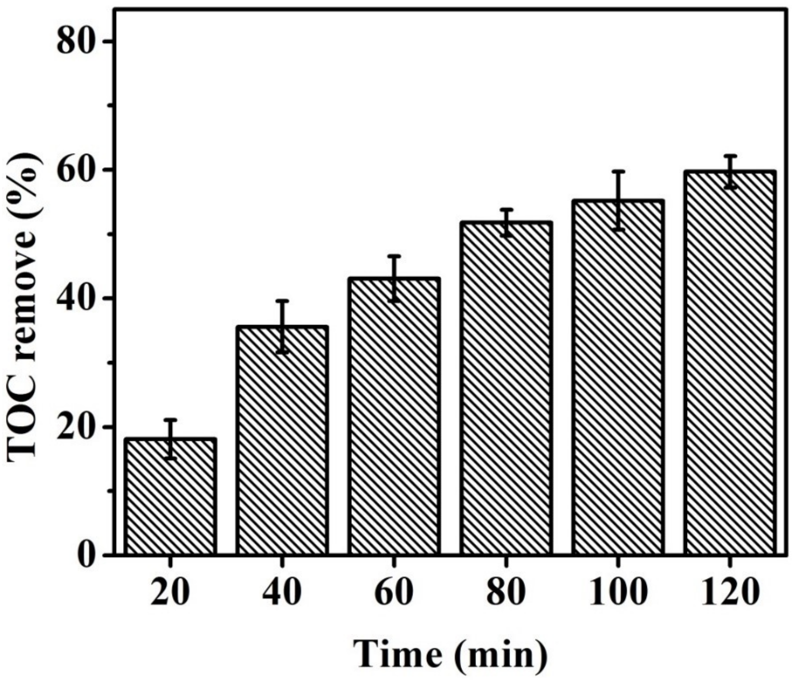

Figure S10. The total organic carbon (TOC) removal efficiency of $ZnO/BiVO_4$-3.

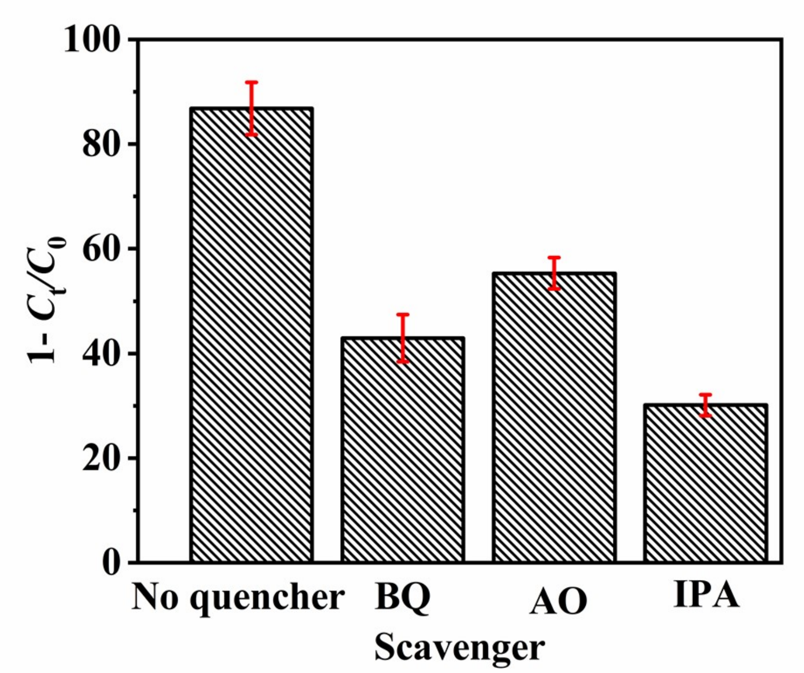

Figure S11. Effects of different scavengers to photocatalytic degradation of CBZ by $ZnO/BiVO_4$-3.

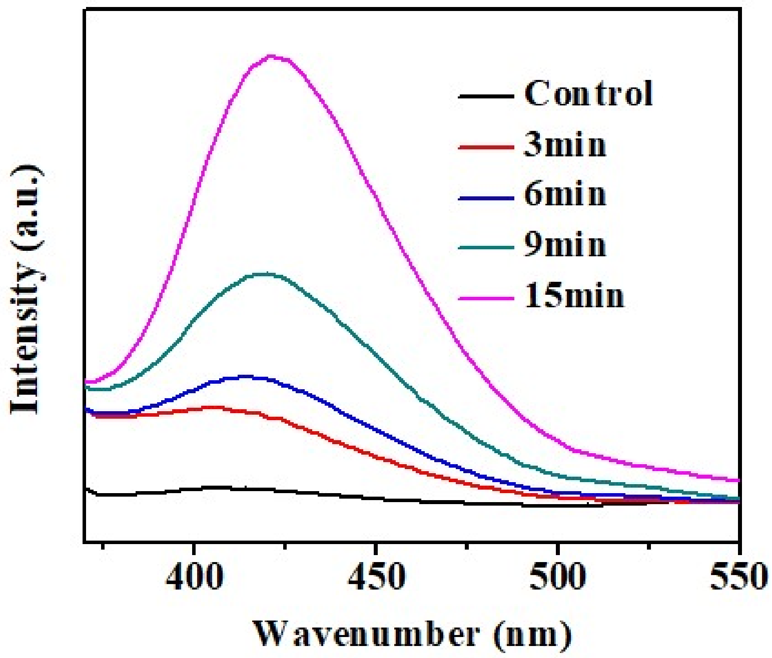

Figure S12. PL spectra of •OH generated in the ZnO/$BiVO_4$-3 aqueous reaction system.

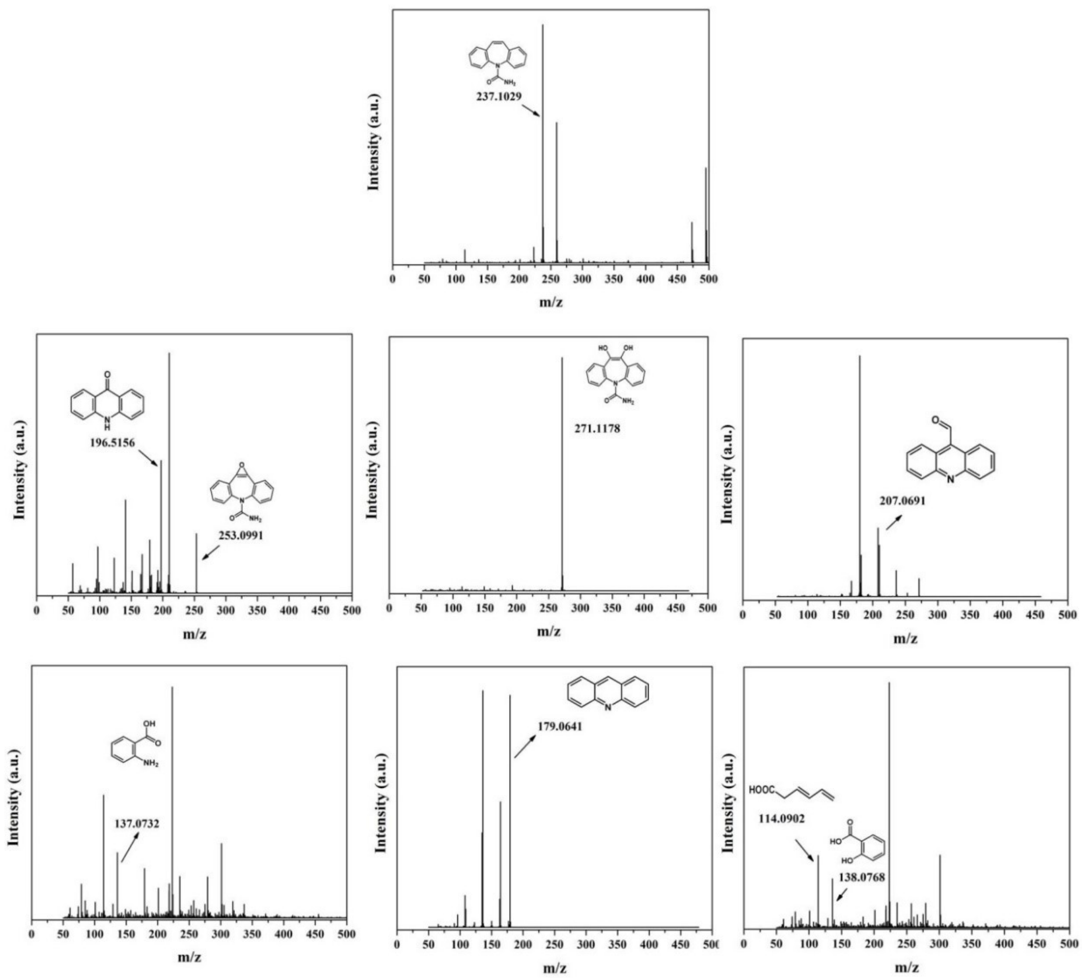

Figure S13. The CBZ and its intermediate product in the degradation process.

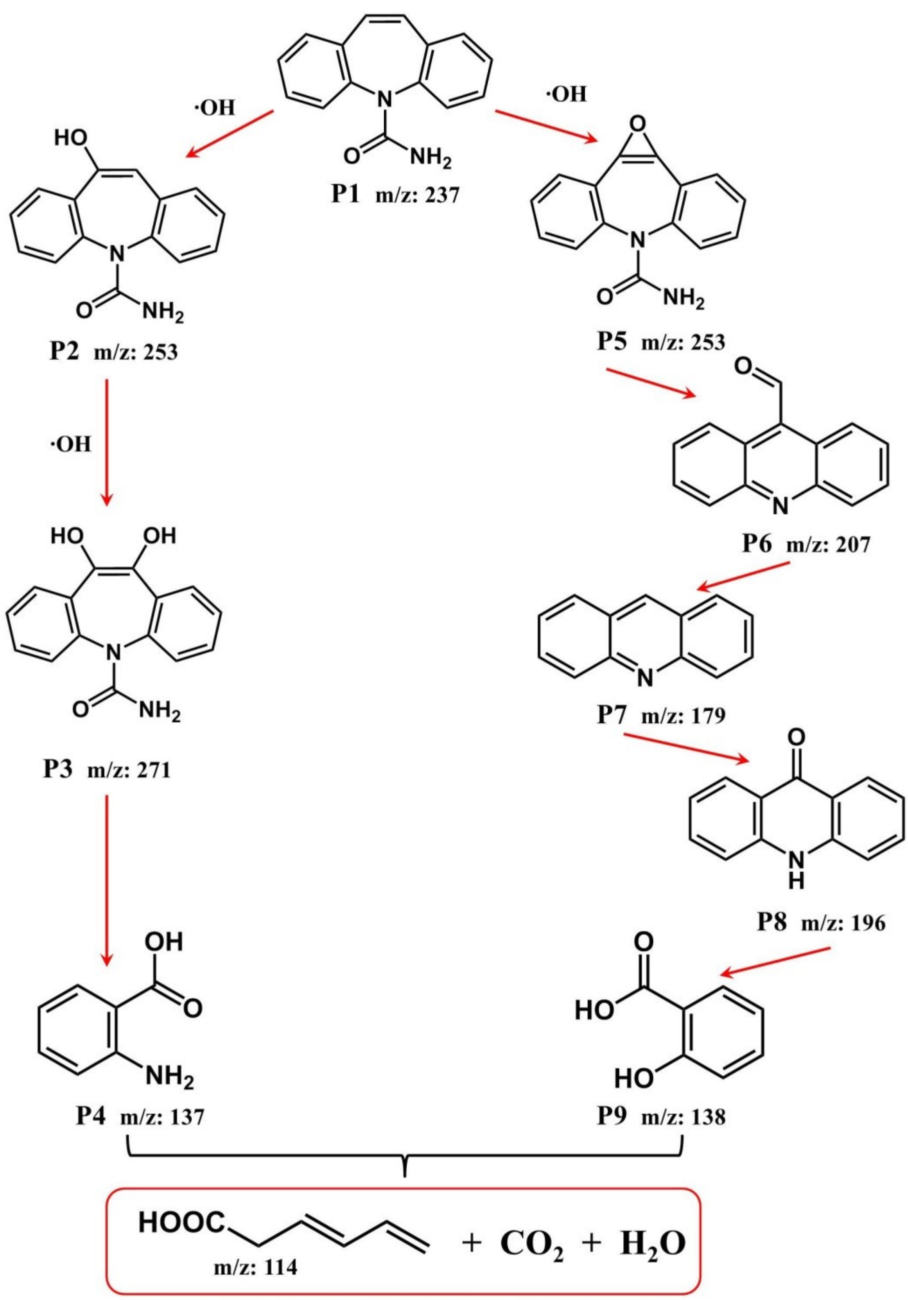

Figure S14. Degradation pathways of CBZ over ZnO/BiVO$_4$-3 composite.

Section 3: Tables

Table S1. Specific surface area and porosity of the samples

Samples	Specific surface area (m^2/g)	Pore volume (cm^3/g)	Average pore diameter (nm)
ZnO	67.26	0.116	26.57
$BiVO_4$	13.17	0.194	186.83
$ZnO/BiVO_4$-3	30.82	0.151	125.62

Table S2. Comparison of CBZ degradation efficiency for different catalysts.

Catalyst	**Reaction condition**	**Reaction time (min)**	**Rate constant (min^{-1})**	**Reference**
Fe-TiO_2	[catalyst] = 0.5 g/L [CBZ] = 9 mg/L	150	0.0129	[1]
BiOBr/CeO_2	[catalyst] = 0.8 g/L [CBZ] = 5 mg/L	120	0.0163	[2]
α-Fe_2O_3(0.3)/MIL-101(Cr)	[catalyst] = 0.2 g/L [CBZ] = 30 mg/L	180	0.0152	[3]
TiO_2/rGO	[catalyst] = 0.05 g/L [CBZ] = 4.5 mg/L	60	0.0156	[4]
Fe_3O_4/BiOBr/BC	[catalyst] = 1 g/L [CBZ] = 10 mg/L	180	0.0177	[5]
Ag/AgCl/$BiVO_4$	[catalyst] = 1.0 g/L [CBZ] = 10 mg/L	240	0.0108	[6]
ZnO/$BiVO_4$-3	[catalyst] = 0.8 g/L [CBZ] = 10 mg/L	120	0.0145	This work

Section 4: References

[1] A. El Mragui, Y. Logvina, L. Pinto da Silva, O. Zegaoui and J. Esteves da Silva, *Materials*, 2019, **12**, 3874.

[2] L.L. Liang, S.W. Gao, J.C. Zhu, L.J. Wang, Y.N. Xiong, X.F. Xia and L.W. Yang, *Chem. Eng. J.*, 2020, **391**, 123599.

[3] Q, Huo, X.R. Qi, J.S. Li, G.Q. Liu, Y. Ning, X.B. Zhang, B.Y. Zhang, Y.F. Fu and S.Y. Liu, *Appl.Catal. B-Environ.*, 2019, **255**, 117751.

[4] A. Joseph and A. Vijayanandan, *Sustain. Mater. Techno.*, 2023, **38**, e00703.

[5] S. Li, Z.W. Wang, X.T. Zhao, X. Yang, G.W. Liang and X.Y. Xie, *Chem. Eng. J.*, 2019, **360**, 600–611.

[6] G. Yentür and M. Dükkanc , *Ultrason. Sonochem.*, 2021, **78**, 105749.